

Electronic Supplementary Information

Bi-metallic [Cu/Co(6mna)₂]_n metal organic chalcogenolate framework as high-performance electro-catalyst for dye-sensitized solar cells: A ligand-assisted bottom-up synthesis

Chun-Wei Lai^{a,+}, Yu-Chien Lee^{a,+}, Yi-Zhen Jiang^a, Chia-Her Lin^a,
Gautam Kumar^b, Michael H. Huang^b, and Chun-Ting Li^{a,*}

^a *Department of Chemistry, National Taiwan Normal University, Taipei 11677, Taiwan;* ^b *Department of Chemistry and Frontier Research Center on Fundamental and Applied Sciences of Matters, National Tsing Hua University, Hsinchu 300044, Taiwan.*

*Corresponding author: Tel.: +886–2–7749–6146;

Fax: +886–2–2932–4249; E-mail: ctli@gapps.ntnu.edu.tw

1. Materials

Conducting substrate: Fluorine-doped tin oxide (FTO, TEC-7, $7 \Omega \text{ sq.}^{-1}$) conducting glass was purchased from NSG America, Inc., New Jersey, USA. Carbon cloth (CC, W0S1002, thickness = 0.36 mm, basic 15 weight = 120 g cm^{-2} , sheet resistance = $0.60 \Omega \text{ sq.}^{-1}$) was bought from CeTech Co., Ltd., Taiwan. **Photoanode:** Titanium (IV) tetraisopropoxide (TTIP, > 98%) and 2-methoxyethanol ($\geq 99.5\%$) were obtained from Sigma Aldrich. Titanium (IV) chloride (TiCl_4 , >99.9%) was obtained from Acros Organics B.V.B.A. Transparent TiO_2 paste (TL paste, Ti-nanoxide HT/SP, 20 nm) and surlyn[®] (SX1170-60, 60 μm) were supplied by Solaronix S.A., Aubonne, Switzerland. Commercial light scattering TiO_2 particles, ST-41 with an averaged diameter of 200 nm, were obtained from Ishihara Sangyo, Ltd., Japan. Poly(ethylene glycol) (PEG, MW~20,000) were purchased from Merck. Cis-diisothiocyanato-bis(2,2'-bipyridyl-4,4'-dicarboxylato) ruthenium (II) bis(tetrabutylammonium) (N719 dye) were supplied by Luminescence Tech. Corp., Taiwan. **Electrolyte:** Lithium iodide (LiI, synthetical grade) and iodine (I_2 , synthetical grade) were purchased from Merck. 1,2-Dimethyl-3-propylimidazolium iodide (DMPII) was procured from Tokyo Chemical Industry Co., Ltd. Guanidinium thiocyanate (GuSCN , $\geq 99\%$) and 4-tert-butylpyridine (tBP, 96%) were bought from Acros. Lithium perchlorate (LiClO_4 , $\geq 98.0\%$) was obtained from Sigma Aldrich. Tris(1,10-phenanthroline)cobalt(II) bis(trifluoromethanesulfonimide) and tris(1,10-phenanthroline)cobalt(III) tri(trifluoromethanesulfonimide) were synthesized in accordance with our previous studies.¹ Bis(2,9-dimethyl-1,10-phenanthroline)copper(I) trifluoromethanesulfonimide and bis(2,9-dimethyl-1,10-phenanthroline)copper(II) bis(trifluoromethanesulfonimide) were synthesized by a reported procedure.² **Solvent:** Acetone (99%) and tert-butyl alcohol (tBA, 96%) were bought from Acros. 3-Methoxypropionitrile (MPN, 99%) was procured from Alfa Aesar. Acetonitrile (MeCN, 99.99%) and dichloromethane (DCM, $\geq 99.8\%$) were received from J. T. Baker. *N,N*-Dimethylformamide (DMF, $\geq 99.8\%$), ethanol (EtOH, 99.5%), and isopropyl alcohol (IPA, 99.5%) were obtained from Sigma Aldrich. **MOF synthesis:** Copper (II) nitrate hydrate ($\text{Cu}(\text{NO}_3)_2 \cdot 2.5\text{H}_2\text{O}$, 98%) was obtained from Honeywell Research Chemicals International Inc., USA. 6,6'-Dithiodinicotinic acid (H_2dtdn , >98%) was obtained from Tokyo Chemical Industry Co., Ltd. Pyrazine (Pyz, >99%) was obtained from Thermo Fisher Scientific Inc. 6-Mercaptopyridine-3-carboxylic acid (6mna, >90%) was obtained from Sigma Aldrich. Cobalt (II) chloride hexahydrate ($\text{CoCl}_2 \cdot 6\text{H}_2\text{O}$) and cobalt (II) nitrate hexahydrate ($\text{Co}(\text{NO}_3)_2 \cdot 6\text{H}_2\text{O}$) were procured from Alfa Aesar.

2. Fabrication of the DSSCs

Conducting substrate, FTO and carbon cloth, were cleaned with a neutral cleaner and then washed with de-ionized water, acetone, and isopropanol sequentially. A mesoporous TiO_2 photoanode (with an working area of 0.20 cm^2) was coated on a cleaned FTO by the following procedures. (1) The first TiO_2 compact layer (~100 nm) was spin-coated on FTO under 3000 rpm for 30 s using a precursor solution of TTIP/2-methoxyethanol with a weight ratio of 1/3. (2) The second TiO_2 transparent layer (~10 μm) was doctor-bladed onto the first layer using the commercial TL paste purchased from Solaronix. (3) The third TiO_2 scattering layer (~4 μm) was doctor-bladed onto the second layer using a reported home-made paste¹. (4) Last, the TiO_2 thin film was treated by a 70 mM of TiCl_4 solution

(with a solvent) at 70 °C for 30 min in a mixing solvent of deionc water/ethanol (v/v=9/1). The TiO₂ layer made by every step would be followed by a sintering process at 500 °C for 30 min in an ambient atmosphere. After the sintering process, the TiO₂ photoanode was immersed in a 5.0×10⁻⁴ M of N719 dye solution using a mixed solvent of MeCN/tBA with a volume ratio of 1:1 at room temperature for 24 h. A TiO₂ photoanode was coupled with a counter electrode made by this work. And the cell gap was maintained by using a 60 μm-thick Surlyn[®] film as the spacer.

3. Material characterizations

Crystallinity and molecular structure of as-synthesized MOF particle were analyzed by powder X-ray diffraction pattern spectroscopy (PXRD, Bruker D8 advance, Billerica, USA) and single crystal X-ray diffraction pattern spectroscopy (SCXRD, Bruker D8 venture, Billerica, USA). Nitrogen-gas (N₂) adsorption-desorption isotherms for various MOF powders were investigated by Micromeritics 3Flex Adsorption Analyzer Georgia USA. Film morphology was observed by field-emission scanning electron microscopy (FE-SEM, Nova NanoSEM 230, FEI, Oregon, USA).

4. Photovoltaic performance measurement

Photovoltaic parameters of the DSSCs with different counter electrodes were obtained by a potentiostat/galvanostat (Metrohm Autolab PGSTAT204, Autolab, Eco-Chemie, the Netherlands) at the simulated solar irradiation (100 mW cm⁻²; AM 1.5G) and Philip desk lamp (Helix 23WD EMI lamp; a correlated color temperature of 6500K; 6, 3, and 1 klux). The simulated solar irradiation was performed by a class A quality solar simulator (PEC-L11, AM1.5G, Peccell Technologies, Inc., Kanagawa, Japan). The incident light intensity was calibrated by a standard Si cell (PECSI01, Peccell Technologies, Inc.) and by an optical detector (model 818-SL, Newport, California, USA) coupled with a power meter (model 1916-R, Newport, California, USA). The DSSC device was composed of a sandwich structure of photoanode/ electrolyte/ counter electrode; where an indential TiO₂ film adsorbed with N719 sensitizer was the photoanode, an liquid iodide-based mixture was the electrolyte, and the different electrodes made by this work were used as the counter electrodes. Here, the iodide-based electrolyte contained 1.2 M DMPII, 0.035 M I₂, 0.1 M GuSCN, and 0.5 M tBP in MPN/MeCN (volume ratio of 1:4) and was injected into the gap between photoanode and counter electrode by capillarity.

5. Cyclic voltammetry (CV) analysis

CV analysis was executed by a potentiostat/galvanostat (Metrohm Autolab PGSTAT204, Autolab, Eco-Chemie, the Netherlands) using a three-electrode system. The sample electrode was used as the working electrode. A Pt foil and Ag/Ag⁺ electrode were used as the auxiliary and reference electrodes, respectively. For the measurements of I⁻/I₃⁻ redox mediator, the iodide-based electrolyte contained 10.0 mM of LiI, 1.0 mM of I₂, and 0.1 M of LiClO₄ in acetonitrile. For the measurements of Co-phen²⁺/Co-phen³⁺ redox mediator, the cobalt-based electrolyte contained 10.0 mM of tris(1,10-phenanthroline)cobalt(II) bis(trifluoromethanesulfonimide), 1.0 mM of tris(1,10-phenanthroline)-cobalt(III) tri(trifluoromethanesulfonimide), and 0.1 M LiClO₄ in acetonitrile. For the measurements

of Cu-dmp⁺/Cu-dmp²⁺ redox mediator, the copper-based electrolyte contained 10.0 mM of bis(2,9-dimethyl-1,10-phenanthroline)copper(I) trifluoromethanesulfonimide, 1.0 mM of bis(2,9-dimethyl-1,10-phenanthroline)copper(II) bis(trifluoromethanesulfonimide), and 0.1 M of LiClO₄ in acetonitrile. The scan rate for CV analysis was performed at 20, 40, 60, 80, or 100 mV s⁻¹.

6. Tafel polarization plot, and electrochemical impedance spectra

Tafel polarization plots and electrochemical impedance spectra (EIS) analyses were recorded a potentiostat/galvanostat (Metrohm Autolab PGSTAT204, Autolab, Eco-Chemie, the Netherlands) equipped with a FRA2 module by using a symmetrical cell structure of electrode/electrolyte/electrode; where an electrode made by this work was applied for both anode and cathode. The electrolyte for Tafel and EIS analyses contained 1.2 M DMPII, 0.035 M I₂, 0.1 M GuSCN, and 0.5 M tBP in MPN/MeCN (volume ratio of 1:4). For Tafel measurement, linear sweep voltammetry (LSV) was performed from 1 V to -1 V at a DC bias with a scan rate of 100 mV s⁻¹. A Tafel polarization curve is presented as a logarithm of current density–voltage ($\log J$ - V) curve, which is generally divided into three zones: (1) the polarization zone for forming an electrical double layer at $|V| < 120$ mV, (2) the Tafel zone for executing charge transfer at $120 \text{ mV} < |V| < 400$ mV, and (3) the diffusion zone for reaching a horizontal limiting current at $|V| > 400$ mV. Accordingly, a linear fitting line is obtained at the anodic or cathodic Tafel zone to find the exchanged current density (J_0 ; mA cm⁻²) at the intercept (at $V = 0$). In a region of $\log |J_0| \pm 0.2$ mA cm⁻², a Tafel slope (β ; mV decade⁻¹) for each sample is acquired by another linear fitting line, which is commonly presented as a voltage–logarithm of current density (V - $\log J$) curve.

For EIS analysis, the data was collected using the same dummy cell as for Tafel analysis under an AC amplitude of ± 10 mV, an AC frequency from 1 Hz to 100 kHz, and an applied bias of 0 V. A Nyquist plot is presented as the imaginary impedance–real impedance ($-Z''$ - Z') spectra, which is typically divided into three regions: (1) high-frequency region of $10^5 \sim 10^4$ Hz at the left-hand-side onset point, referring to the series resistance (R_s) at the electro-catalytic film/substrate interface; (2) middle-frequency region of $10^4 \sim 10^3$ Hz for collecting the radius of the left-hand-side semi-circle, referring to the charge transfer resistance (R_{ct}) at the electro-catalytic film/electrolyte interface; (3) low-frequency region of $10^3 \sim 10^0$ Hz for getting the diameter of right-hand-side semi-circle, referring to Warburg diffusion resistance (Z_w) within the electrolyte layer.

Table S1 A partial list of the DSSC performance with MOF-based counter electrodes, based on the device using a photoanode of TiO₂/N719 and an I⁻/I₃⁻ electrolyte.

Ligands	Counter Electrode	η [%]	η of Pt [%]	Ref.
<u>Imidazole</u>	FTO/ZIF-67/ethyl cellulose	2.9	7.9	3
	FTO/ZIF-67 derived CoS ₂ /carbon nanocage	8.2		
	FTO/ZIF-67 derived CoTe ₂ /N-doped CNT-grafted polyhedron	9.0	8.0	4
	FTO/ZIF-67 derived CoTe ₂ /N-doped graphitic carbon-coated polyhedron	8.6		
	FTO/ZIF-67 derived Co-doped MoS _x hollow nanobox	9.6	8.4	5
	FTO/ ZIF-67 derived CoSe ₂ /N-doped CNT	9.3	7.8	6
	FTO/(ZIF-8/ZIF-67) derived Ni/Co-embedded N-doped carbon polyhedron/CNT	8.8	7.3	7
	FTO/ZIF-8/PEDOT:PSS	7.0	7.2	8
	FTO/ZIF-8/PEDOT:PSS	5.7	8.5	9
	FTO/(ZIF-8@SiO ₂) derived yolk-shell (N-doped carbon@SiO ₂)/PEDOT:PSS	10.0		
	FTO/ZIF-8 derived N-doped carbon	8.3	8.9	10
	FTO/(ZIF-8@polydopamine) derived N-doped carbon	9.0		
	FTO/ZIF-7/PEDOT:PSS	5.3	8.3	11
FTO/ZIF-7 derived ZnSe/N-doped carbon cube/PEDOT:PSS	8.7			
<u>BDC (or BTC)</u>	FTO/Co-BDC derived CoSe ₂ (spin-coated)	6.9	6.4	12
	FTO/Co-BDC derived CoSe ₂ (bottom-up grown)	5.8		
	FTO/Zn-BTC derived ZnO-doped carbon	7.7	9.4	13
	FTO/(Co-BTC/Ni-BTC) derived carbon decorated Co/Ni alloy	9.3	8.0	14
<u>TCPP</u>	FTO/Co-TCPP derived CoS _{1.097} @N-doped carbon	9.1	8.0	15
	CC/Zr-TCPP/s-PT	8.9	8.2	16
	FTO/annealed Zn-TCPP	5.6	6.7	17
<u>Mercaptopicotinate</u>	FTO/[Cu ₂ (6mna)(6mn)NH ₄] _n /PEDOT	8.3	7.7	18
	CC/[Cu ₂ (6mna)(6mn)NH ₄] _n /PEDOT	9.5	N.A.	
	CC/[Cu ₂ (6mna)(6mn)NH ₄] _n -NO ₃	9.4	9.3	This work
	CC/[Co ₂ (6mna) ₂] _n -NO ₃	9.4		
	CC/[Co ₂ (6mna) ₂] _n -Cl	9.9		
	CC/[Cu/Co(6mna) ₂] _n -NO ₃	9.8		
	CC/[Cu/Co(6mna) ₂] _n -Cl	10.0		

CNT= carbon nanotube; PEDOT= poly(3,4-ethylenedioxythio-phenene); PEDOT:PSS= poly(3,4-ethylenedioxythio-phenene): poly(styrene-sulfonate); s-PT= sulfonated-poly(thiophene-3-[2-(2-methoxyethoxy) ethoxy]-2,5-diyI); 6mna= 6-mercaptionicotinic acid; 6mn= 6-mercaptionicotinate.

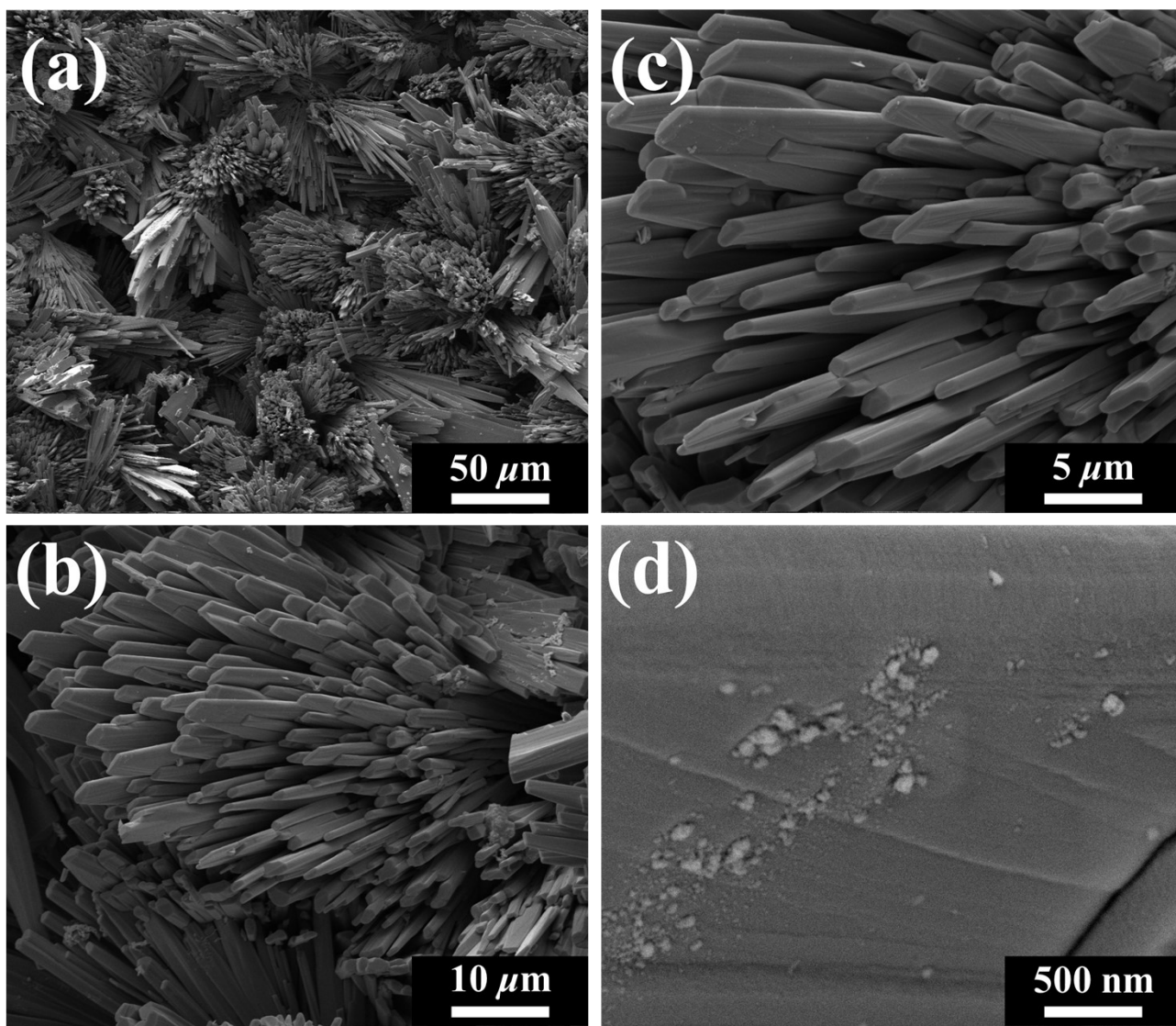


Fig. S1 FE-SEM images of the $\text{CC}/[\text{Cu}_2(6\text{mna})(6\text{mn})\text{NH}_4]_n\text{-NO}_3$ electrode synthesized by 72 h, recorded at the magnification of (a) 1 k, (b) 5 k, (c) 10 k, and (d) 100 k.

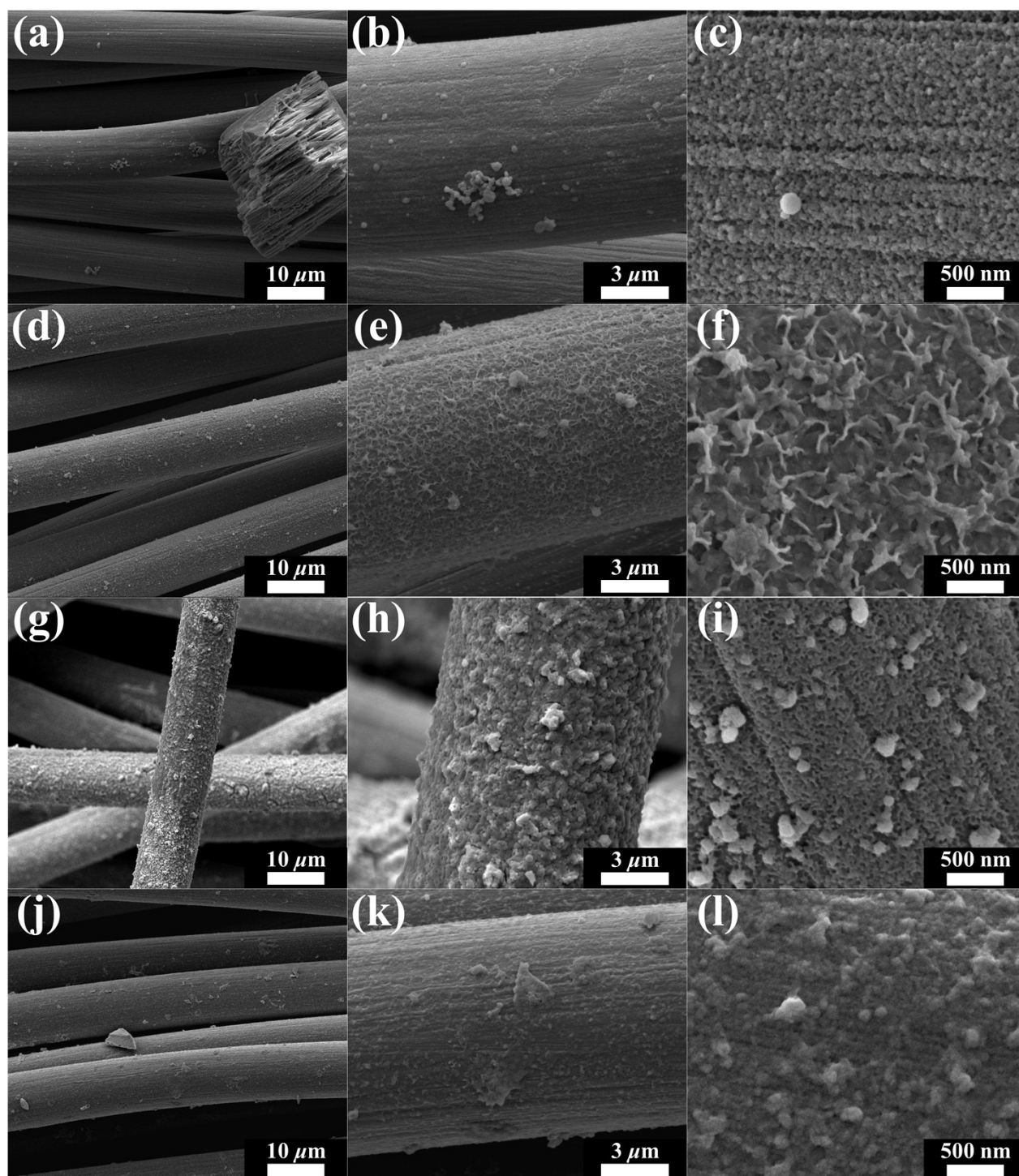


Fig. S2 FE-SEM images of various $\text{CC}/[\text{Co}_2(6\text{mna})_2]_n\text{-NO}_3$ electrodes, synthesized by the reaction time of (a-c) 20, (d-f) 48, (g-i) 72, and (j-l) 96 h.

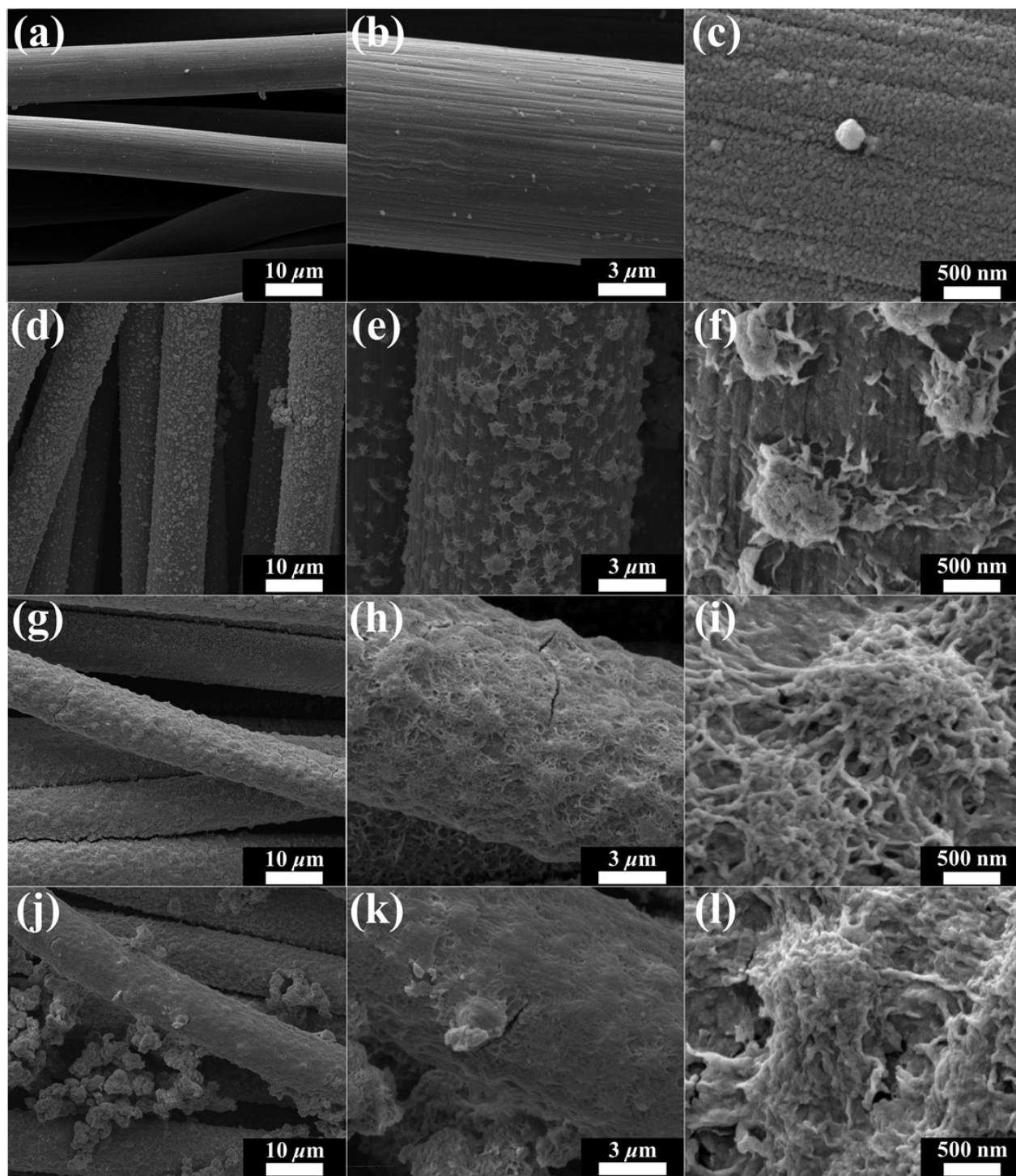


Fig. S3 FE-SEM images of various $\text{CC}/[\text{Co}_2(6\text{-mna})_2]_n\text{-Cl}$ electrodes, synthesized by the reaction time of (a-c) 20, (d-f) 48, (g-i) 72, and (j-l) 96 h.

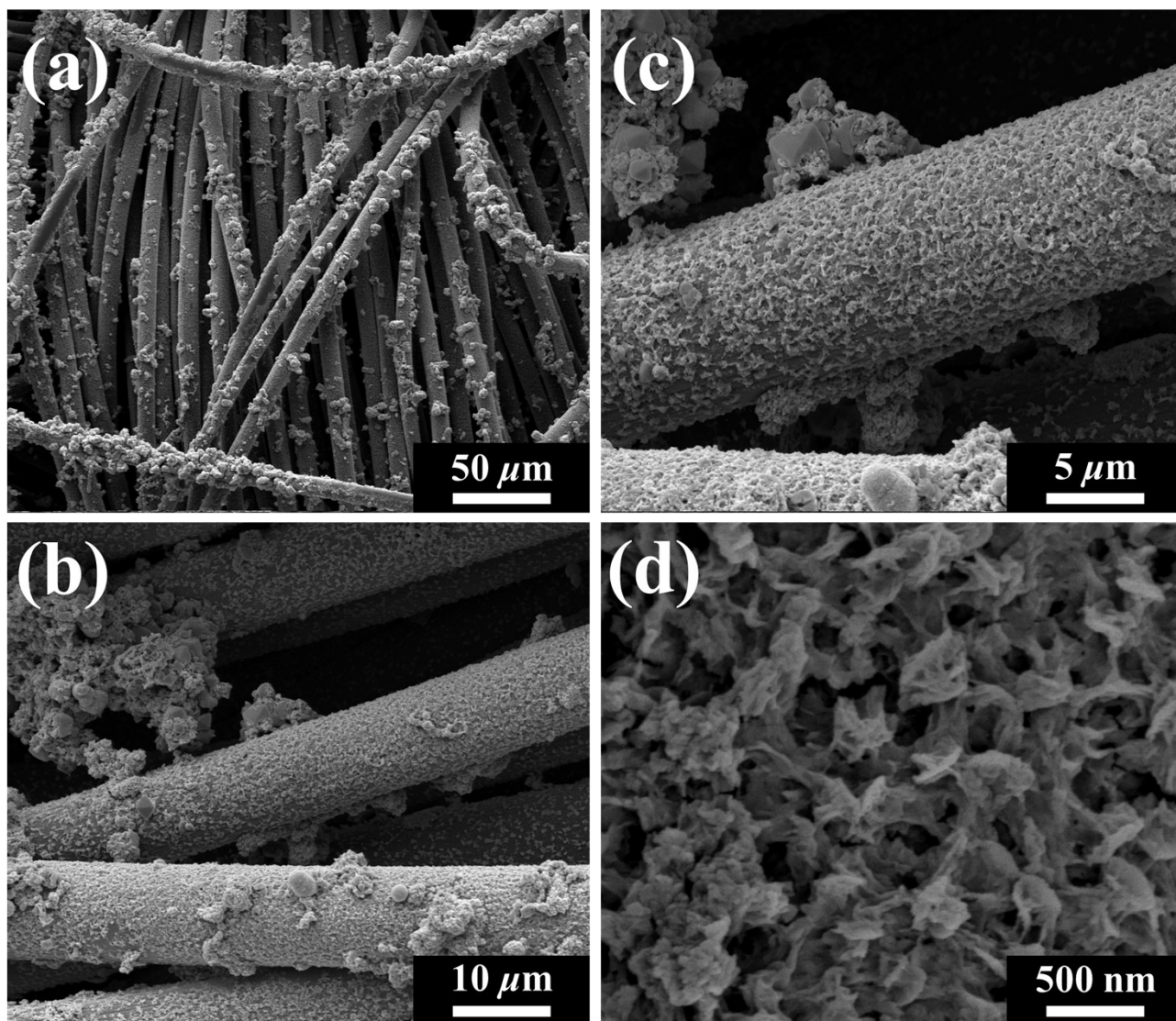


Fig. S4 FE-SEM images of the $\text{CC}/[\text{Cu}/\text{Co}(\text{6mna})_2]_n\text{-NO}_3$ electrode synthesized by 72 h, recorded at the magnification of (a) 1 k, (b) 5 k, (c) 10 k, and (d) 100 k.

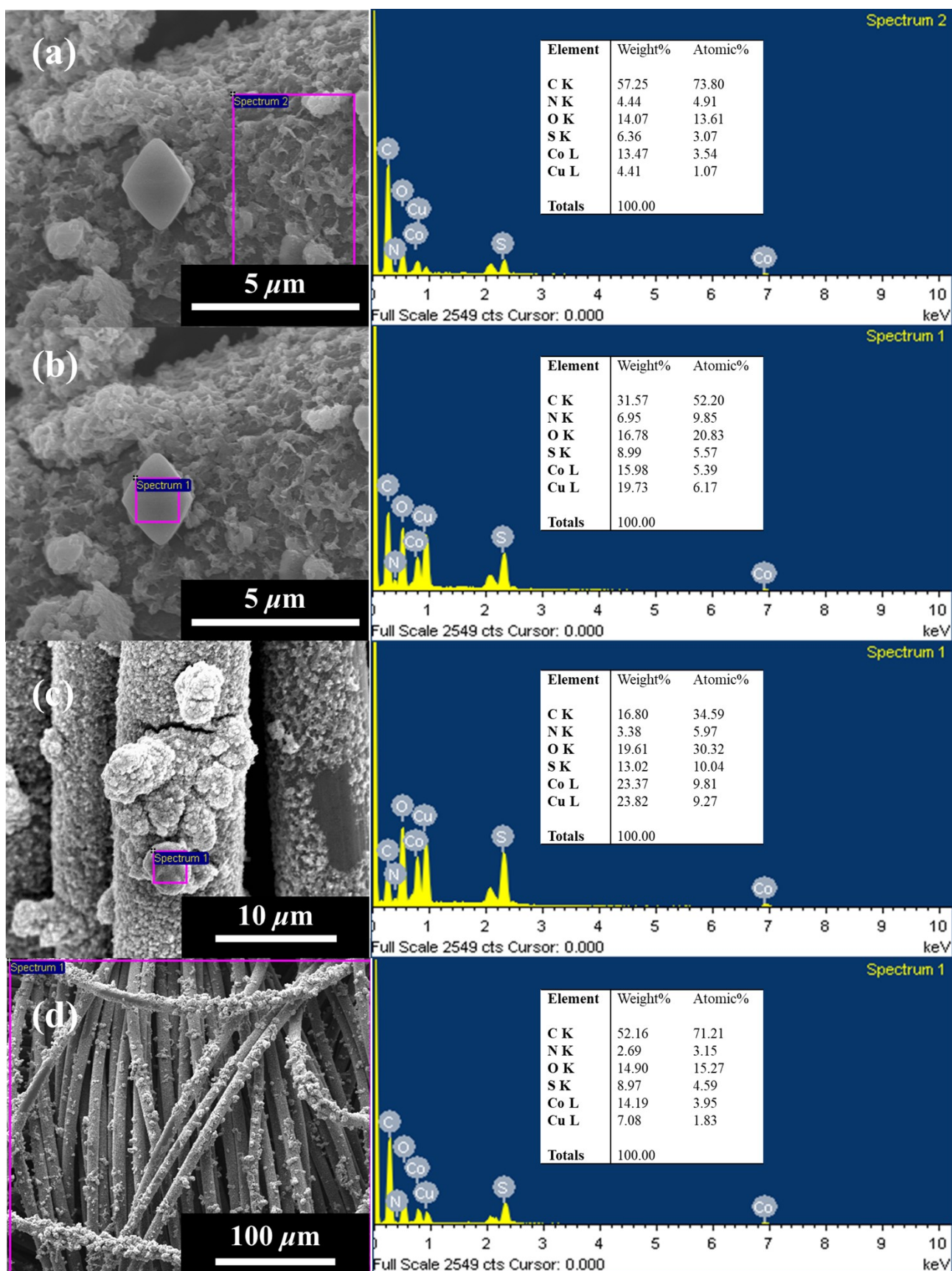


Fig. S5 EDAX spectra of the $\text{CC}/[\text{Cu}/\text{Co}(\text{6mna})_2]_n\text{-NO}_3$ electrode synthesized by 72 h, recorded at (a) silk-like particles, (b) sharp octahedrons, (c) irregular chunks, and (d) bulk film.

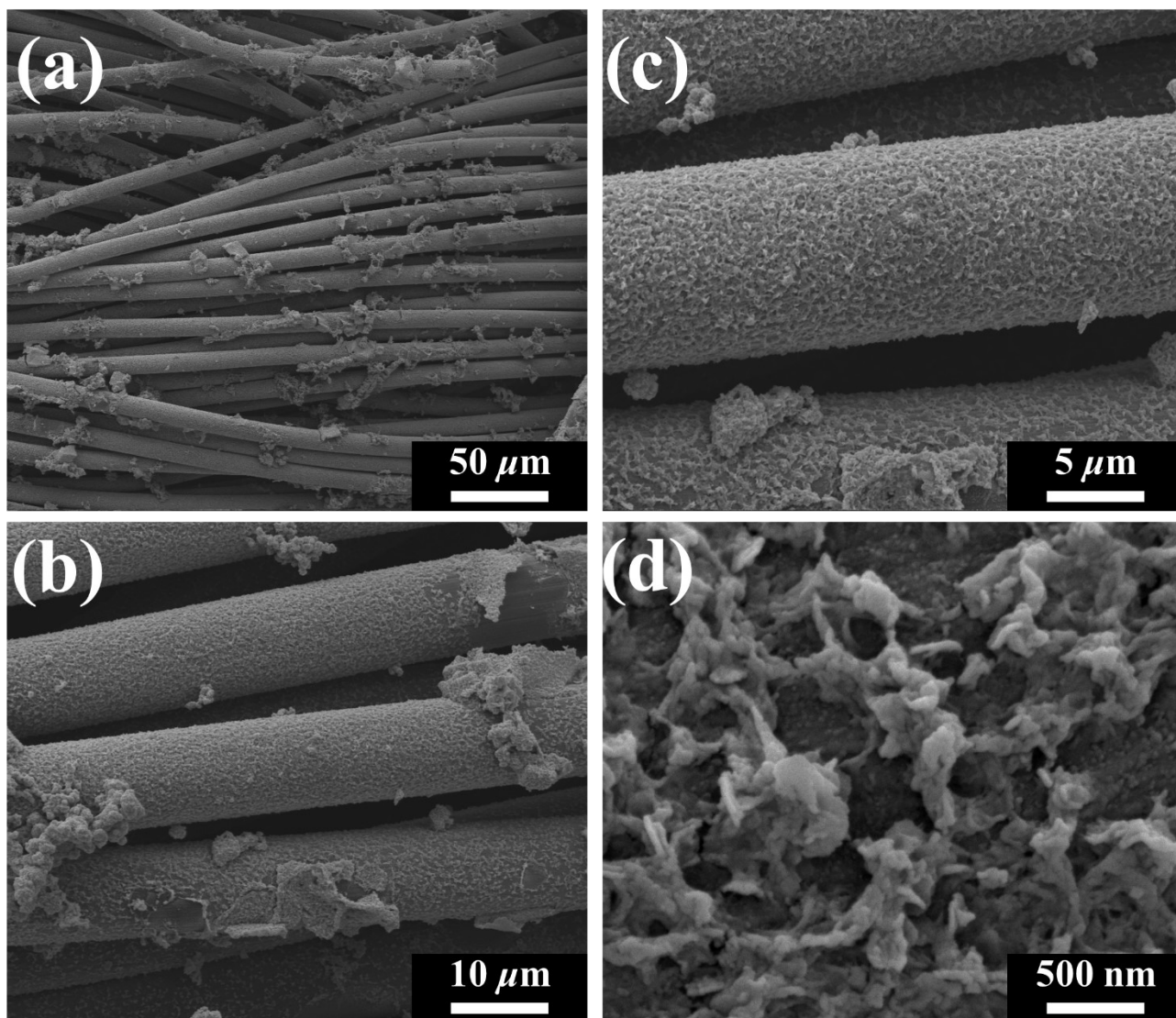


Fig. S6 FE-SEM images of the CC/[Cu/Co(6mna)₂]_n-Cl electrode synthesized by 72 h, recorded at the magnification of (a) 1 k, (b) 5 k, (c) 10 k, and (d) 100 k.

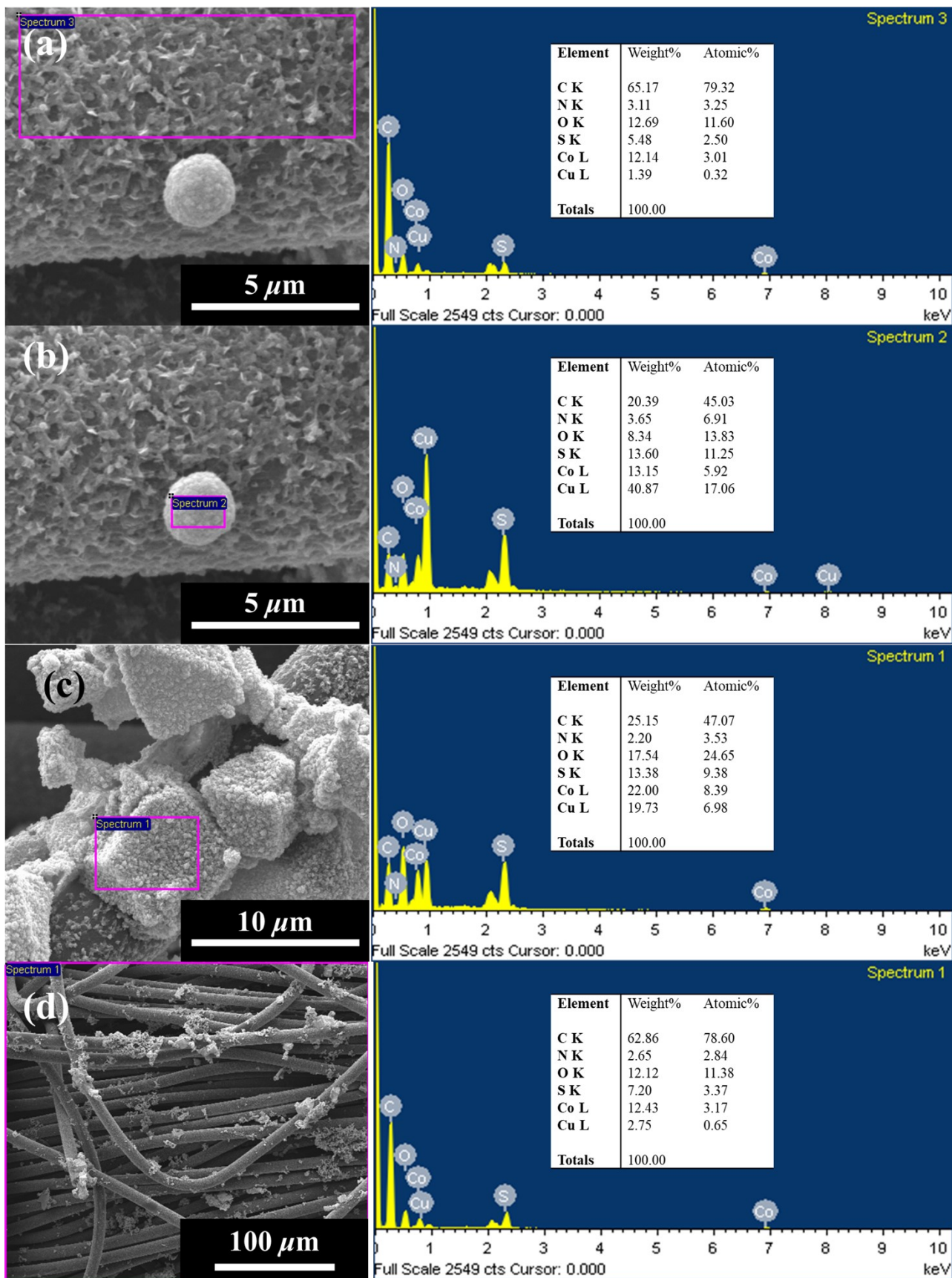


Fig. S7 EDAX spectra of the CC/[Cu/Co(6mna)₂]_n-Cl electrode synthesized by 72 h, recorded at (a) flower-like particles, (b) spherical particles, (c) irregular aggregations, and (d) bulk film.

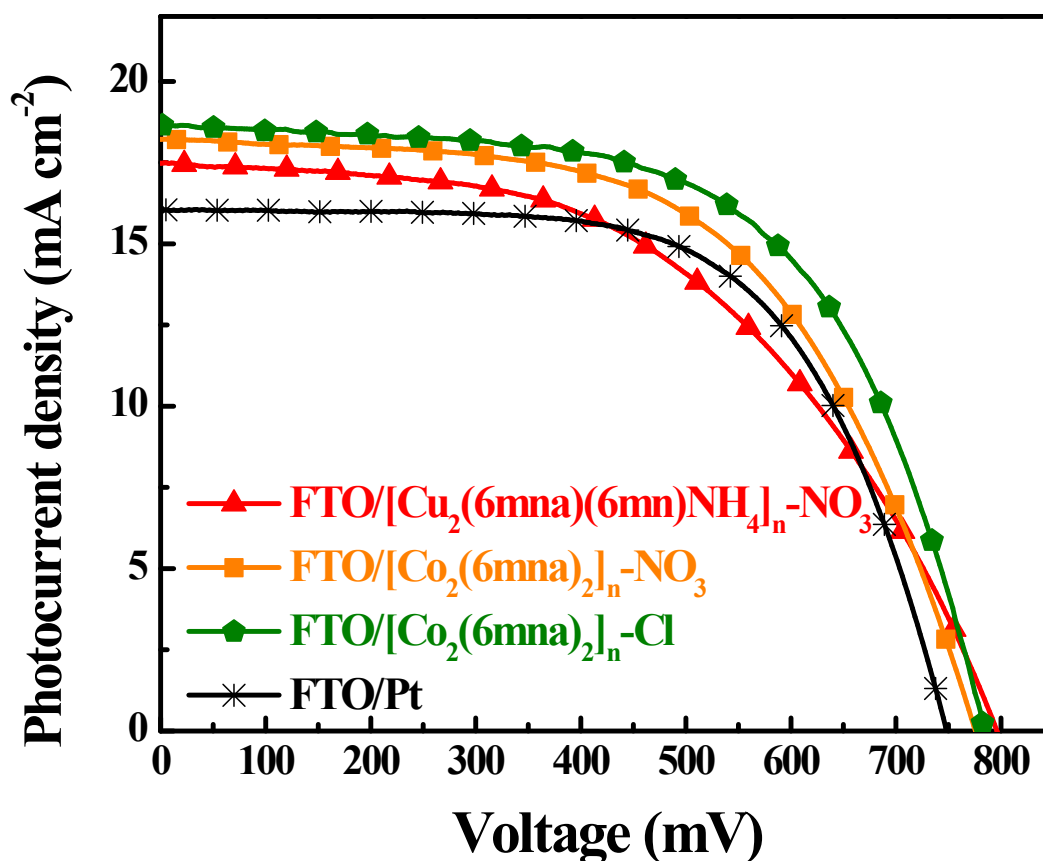


Fig. S8 Photocurrent density–voltage curves of DSSCs coupled with various counter electrodes of FTO/[Cu₂(6mna)(6mn)NH₄]_n-NO₃, CC/[Co₂(6mna)₂]_n-NO₃, FTO/[Cu/Co(6mna)₂]_n-NO₃, and FTO/Pt, measured at a simulated AM 1.5G solar illumination (100 mW cm⁻², AM 1.5G).

Table S2 Photovoltaic parameters of DSSCs coupled with various counter electrodes of FTO/[Cu₂(6mna)(6mn)NH₄]_n-NO₃, CC/[Co₂(6mna)₂]_n-NO₃, FTO/[Cu/Co(6mna)₂]_n-NO₃, and FTO/Pt. The standard deviation data for each sample is measured at the simulated solar irradiation (100 mW cm⁻², AM 1.5G) using ten independent devices.

Electrode	η (%)	V_{oc} (mV)	J_{sc} (mA cm ⁻²)	FF
FTO/[Cu ₂ (6mna)(6mn)NH ₄] _n -NO ₃	7.1 ± 0.4	800 ± 90	17.3 ± 0.4	0.52 ± 0.02
FTO/[Co ₂ (6mna) ₂] _n -NO ₃	8.1 ± 0.1	780 ± 10	18.2 ± 0.2	0.58 ± 0.01
FTO/[Co ₂ (6mna) ₂] _n -Cl	8.8 ± 0.3	780 ± 120	18.6 ± 0.3	0.61 ± 0.01
FTO/Pt	7.7 ± 0.0	750 ± 20	16.1 ± 0.1	0.64 ± 0.01

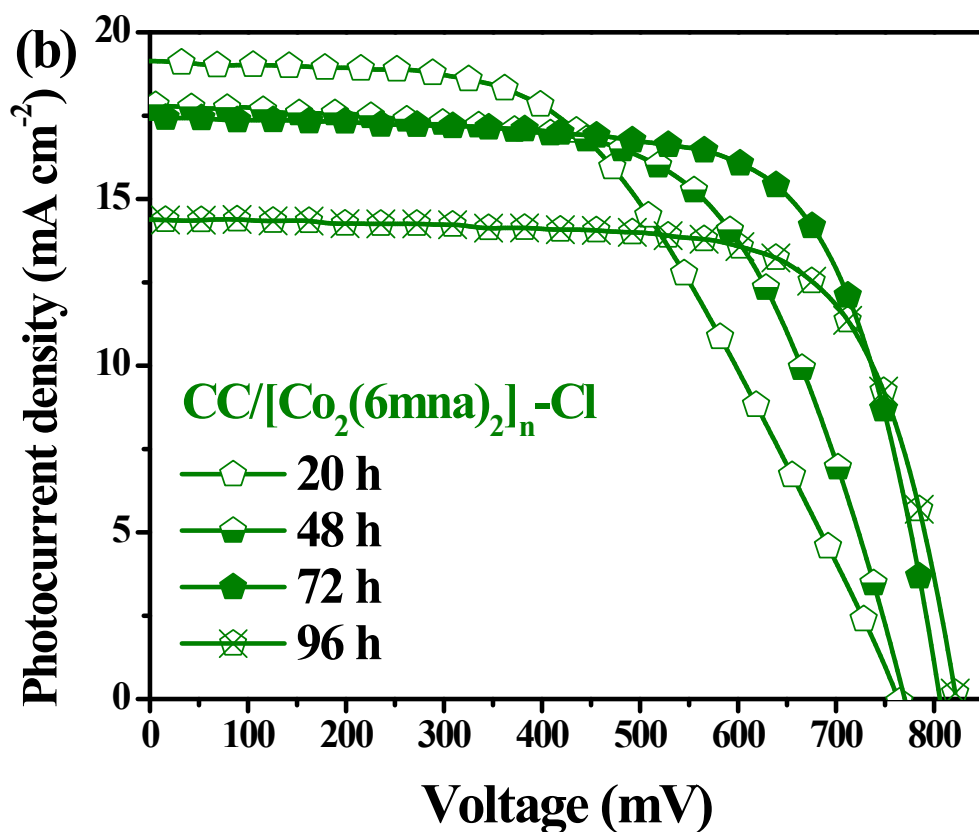
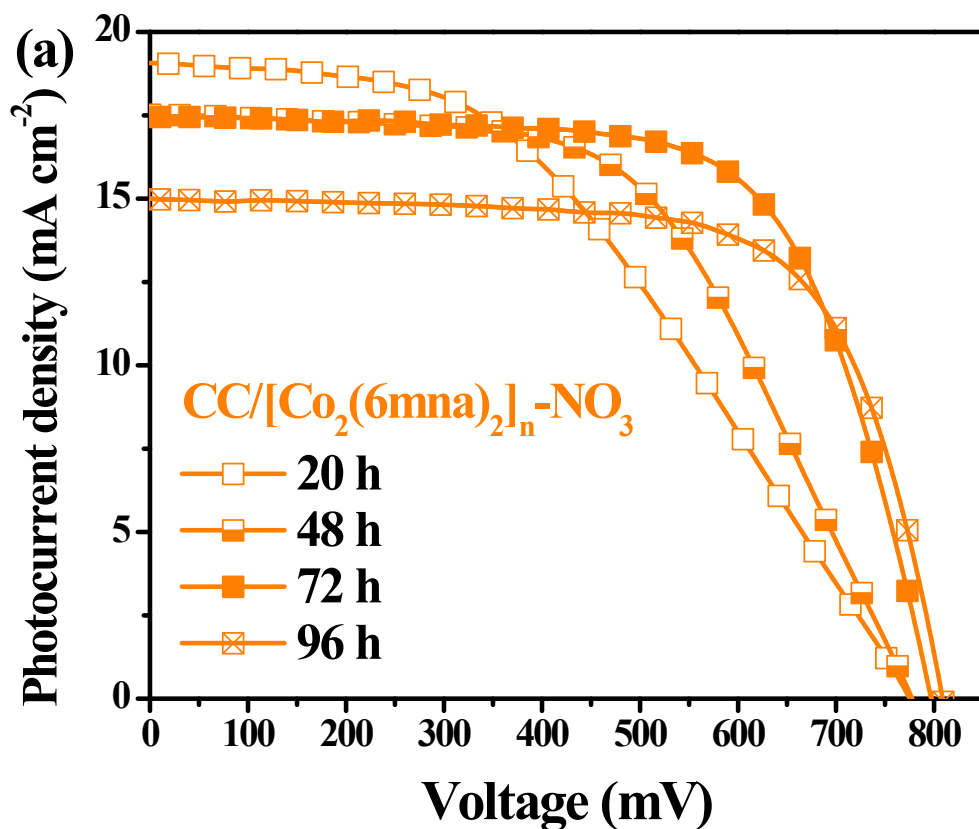


Fig. S9 Photocurrent density–voltage curves of DSSCs coupled with the counter electrodes of (a) various $CC/[Co_2(6mna)_2]_n-NO_3$ and (b) various $CC/[Co_2(6mna)_2]_n-Cl$, synthesized by different reaction times (20, 48, 72, and 96 h).

Table S3 Photovoltaic parameters of DSSCs coupled with the counter electrodes of various CC/[Co₂(6mna)₂]_n-NO₃ and CC/[Co₂(6mna)₂]_n-Cl, synthesized by different reaction times.

Electrode	Reaction time (h)	η (%)	V_{oc} (mV)	J_{sc} (mA cm ⁻²)	FF
CC/[Co ₂ (6mna) ₂] _n -NO ₃	20	6.5 ± 0.2	770 ± 130	19.0 ± 0.3	0.44 ± 0.00
	48	7.8 ± 0.1	780 ± 140	17.6 ± 0.4	0.57 ± 0.02
	72	9.4 ± 0.1	800 ± 20	17.4 ± 0.1	0.68 ± 0.00
	96	8.6 ± 0.4	810 ± 140	15.1 ± 0.6	0.70 ± 0.00
CC/[Co ₂ (6mna) ₂] _n -Cl	20	7.5 ± 0.3	760 ± 150	19.0 ± 0.3	0.52 ± 0.01
	48	8.5 ± 0.3	770 ± 140	17.9 ± 0.5	0.62 ± 0.01
	72	9.9 ± 0.3	800 ± 50	17.5 ± 0.5	0.71 ± 0.01
	96	8.6 ± 0.5	820 ± 90	14.5 ± 0.7	0.72 ± 0.00

Table S4 Photovoltaic parameters of the DSSCs coupled with the CC/[Cu/Co(6mna)₂]_n-Cl counter electrodes, measured by a Philip desk lamp (Helix 23WD EMI) illumination at 0.5, 1.0, 3.0, and 6.0 klux. The standard deviation for each data is based on five independent devices.

Irradiance (mW cm ⁻²)	η (%)	V_{oc} (mV)	J_{sc} (mA cm ⁻²)	FF
0.16 (0.5 klux)	12.2 ± 0.1	580 ± 10	0.05 ± 0.00	0.66 ± 0.01
0.32 (1.0 klux)	19.5 ± 0.1	620 ± 0	0.15 ± 0.00	0.66 ± 0.00
0.97 (3.0 klux)	23.3 ± 0.1	660 ± 10	0.51 ± 0.00	0.67 ± 0.00
1.95 (6.0 klux)	26.4 ± 0.3	680 ± 10	1.14 ± 0.02	0.66 ± 0.01

Table S5 Electrochemical properties of the electrodes of CC/[Cu/Co(6mna)₂]_n-NO₃, CC/[Cu/Co(6mna)₂]_n-Cl, and CC/Pt in an iodide-based electrolyte at a scan rate of 10 mV s⁻¹.

Electrode	J_{pc} [mA cm ⁻²]	E_{sep} [mV]
CC/[Cu/Co(6mna) ₂] _n -NO ₃	0.9	417
CC/[Cu/Co(6mna) ₂] _n -Cl	1.2	306
CC/Pt	0.8	474

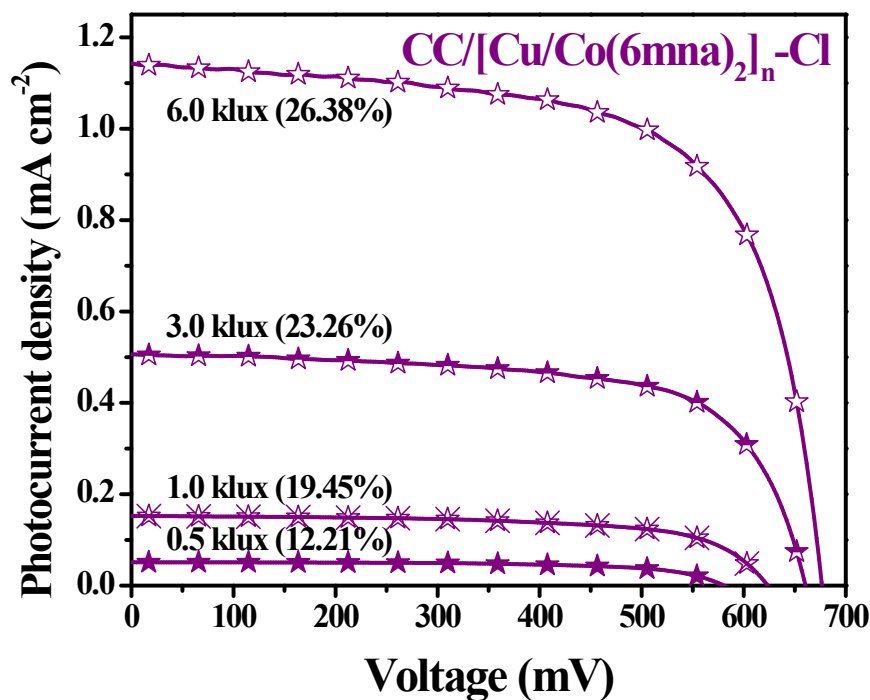


Fig. S10 Photocurrent density–voltage curves of the DSSCs coupled the optimal $\text{CC}/[\text{Cu}/\text{Co}(\text{6mna})_2]_n\text{-Cl}$ counter electrodes, measured at room light illumination (Philips TL5, 14W, 6500K).

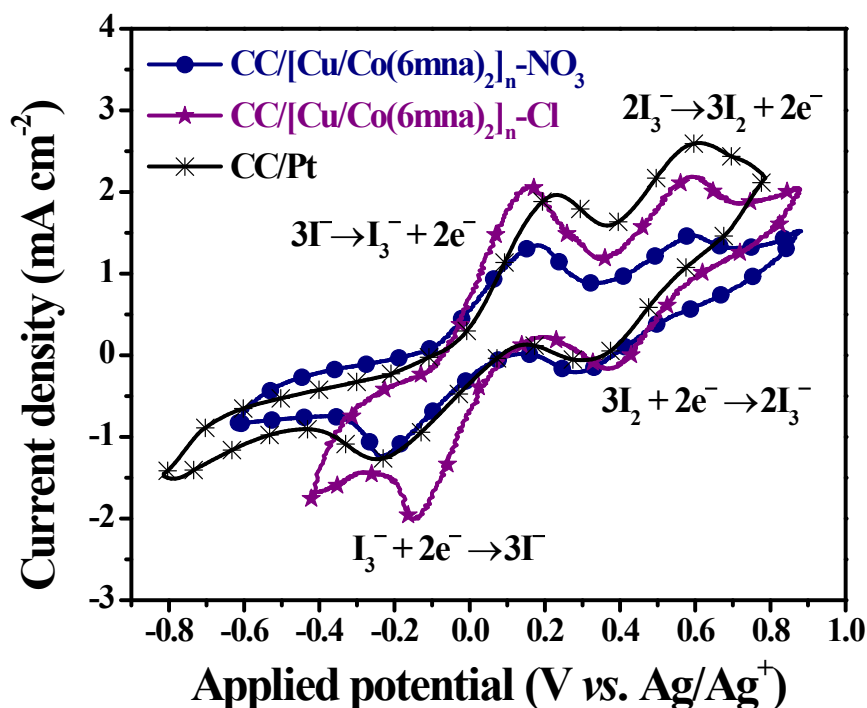


Fig. S11 Cyclic voltammograms of $\text{CC}/[\text{Cu}/\text{Co}(\text{6mna})_2]_n\text{-NO}_3$, $\text{CC}/[\text{Cu}/\text{Co}(\text{6mna})_2]_n\text{-Cl}$, and CC/Pt electrodes, measured in an iodide-based electrolyte at a scan rate of 10 mV s^{-1} .

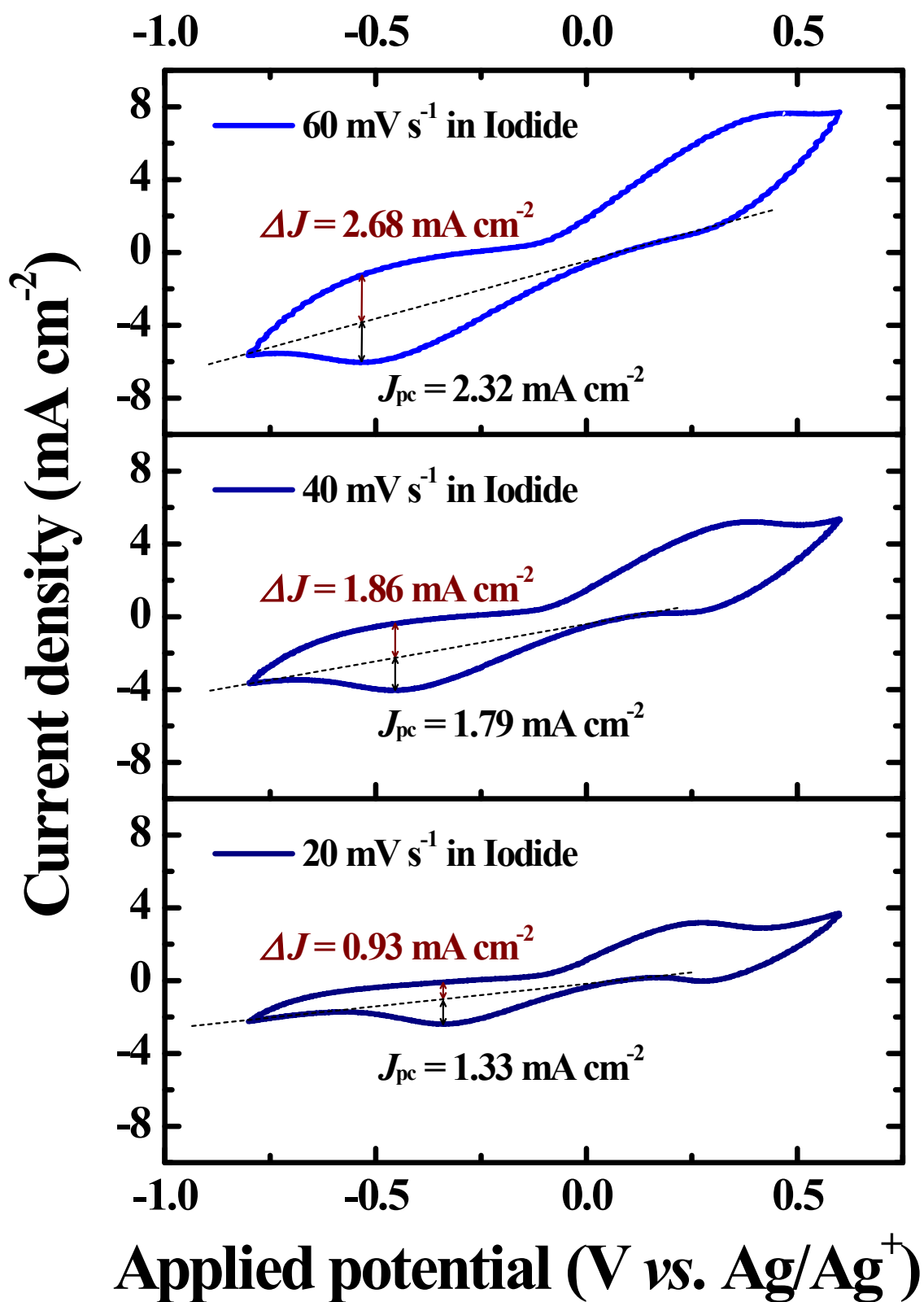


Fig. S12 Cyclic voltammograms of CC/[Cu/Co(6mna)₂]_n-Cl electrode, measured in an iodide-based electrolyte at various scan rates (20, 40, and 60 mV s⁻¹).

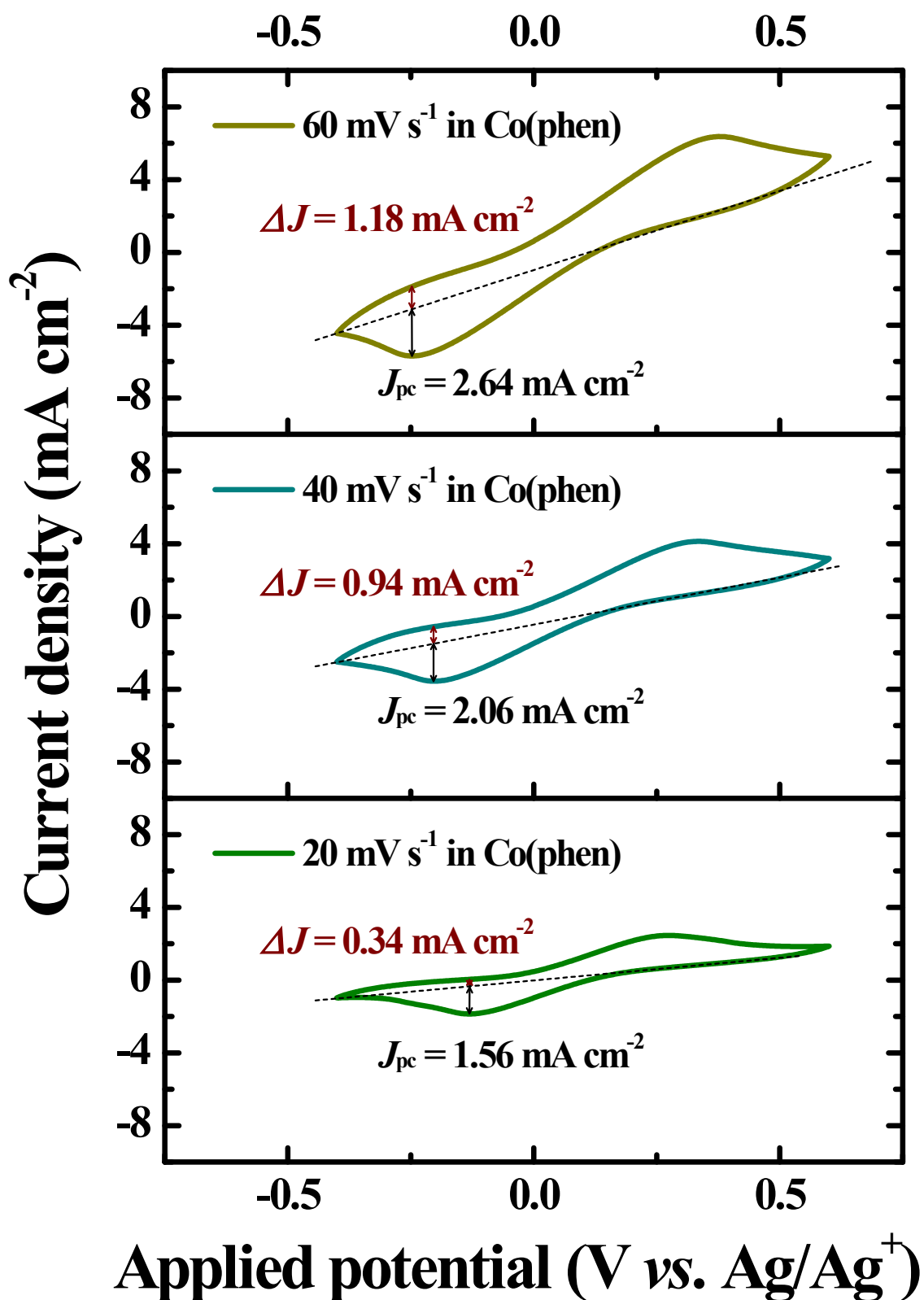


Fig. S13 Cyclic voltammograms of CC/[Cu/Co(6mna)₂]_n-Cl electrode, measured in an Co(phen)-based electrolyte at various scan rates (20, 40, and 60 mV s⁻¹).

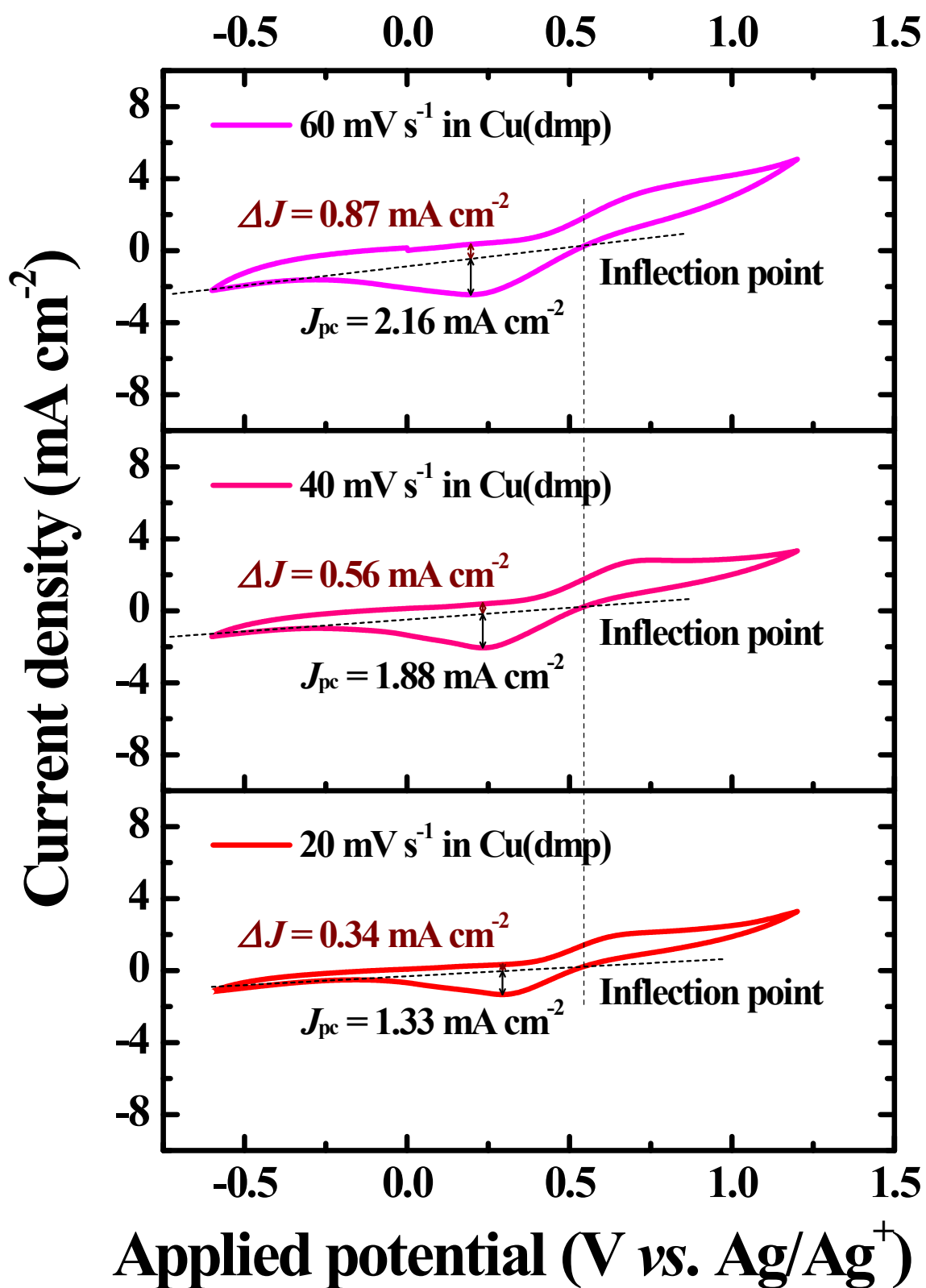


Fig. S14 Cyclic voltammograms of CC/[Cu/Co(6mna)₂]_n-Cl electrode, measured in an Cu(dmp)-based electrolyte at various scan rates (20, 40, and 60 mV s⁻¹).

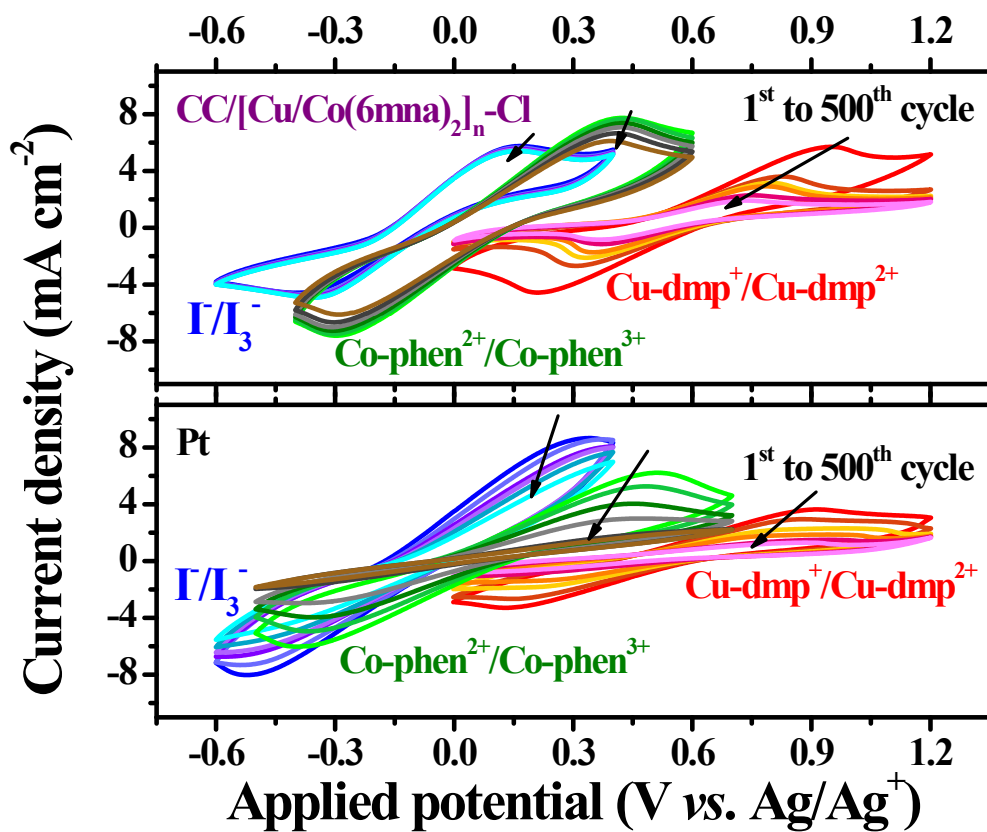


Fig. S15 Long-term cyclic voltammograms of the CC/[Cu/Co(6mna)₂]_n-Cl and CC/Pt electrodes, measured at 100 mV s⁻¹ in an iodide-based (blue), cobalt-based (green), or copper-based (red) electrolytes.

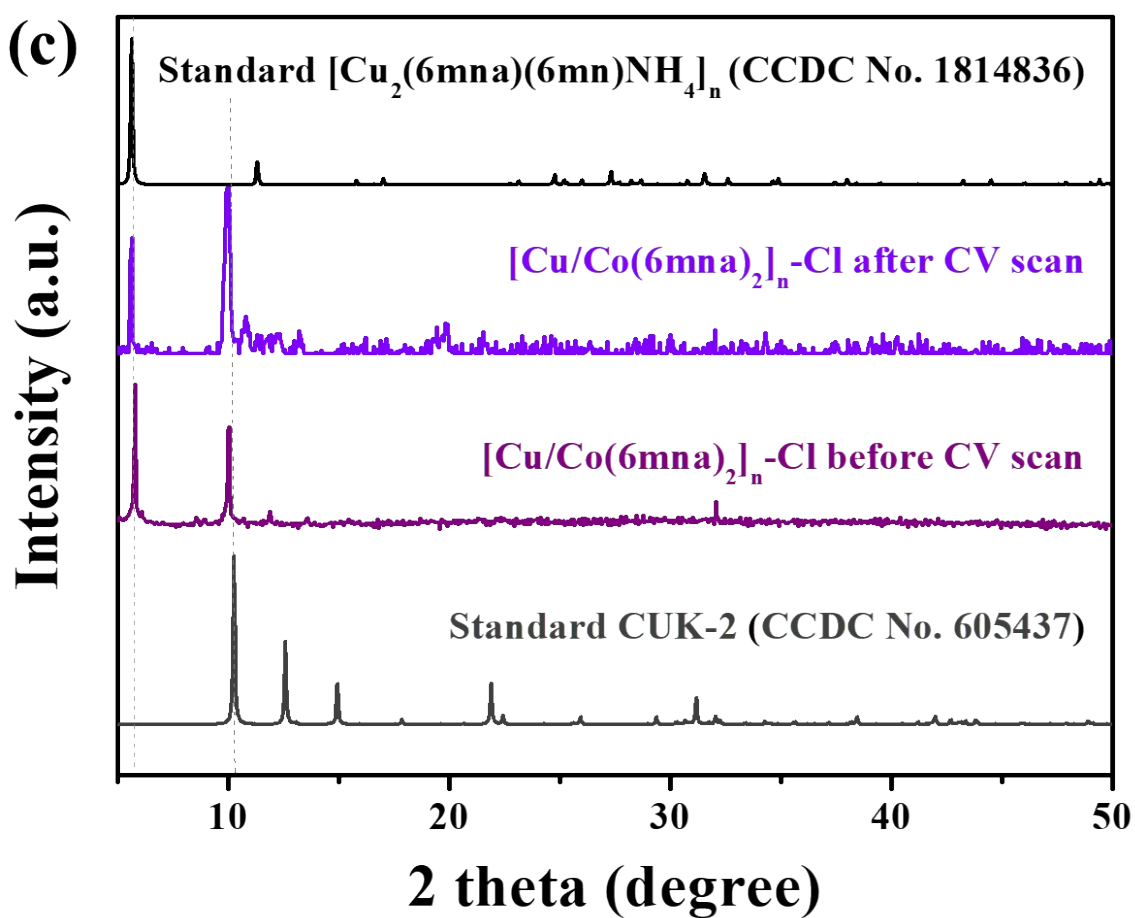
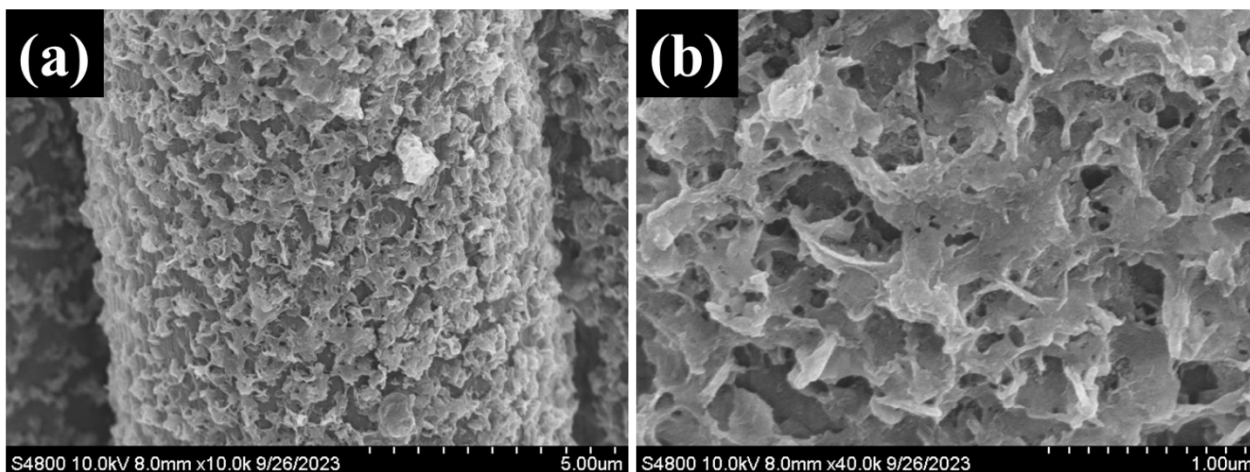


Fig. S16 FE-SEM images of the CC/[Cu/Co(6mna)₂]_n-Cl electrode synthesized by 72 h, recorded after 500 cycles of CV scanning at the magnification of (a) 10 k and (b) 40 k. (c) Powder X-ray diffraction patterns of [Cu/Co-(6mna)₂]_n-Cl before (purple line) and after (violet line) long-term CV scan in I⁻/I₃⁻.

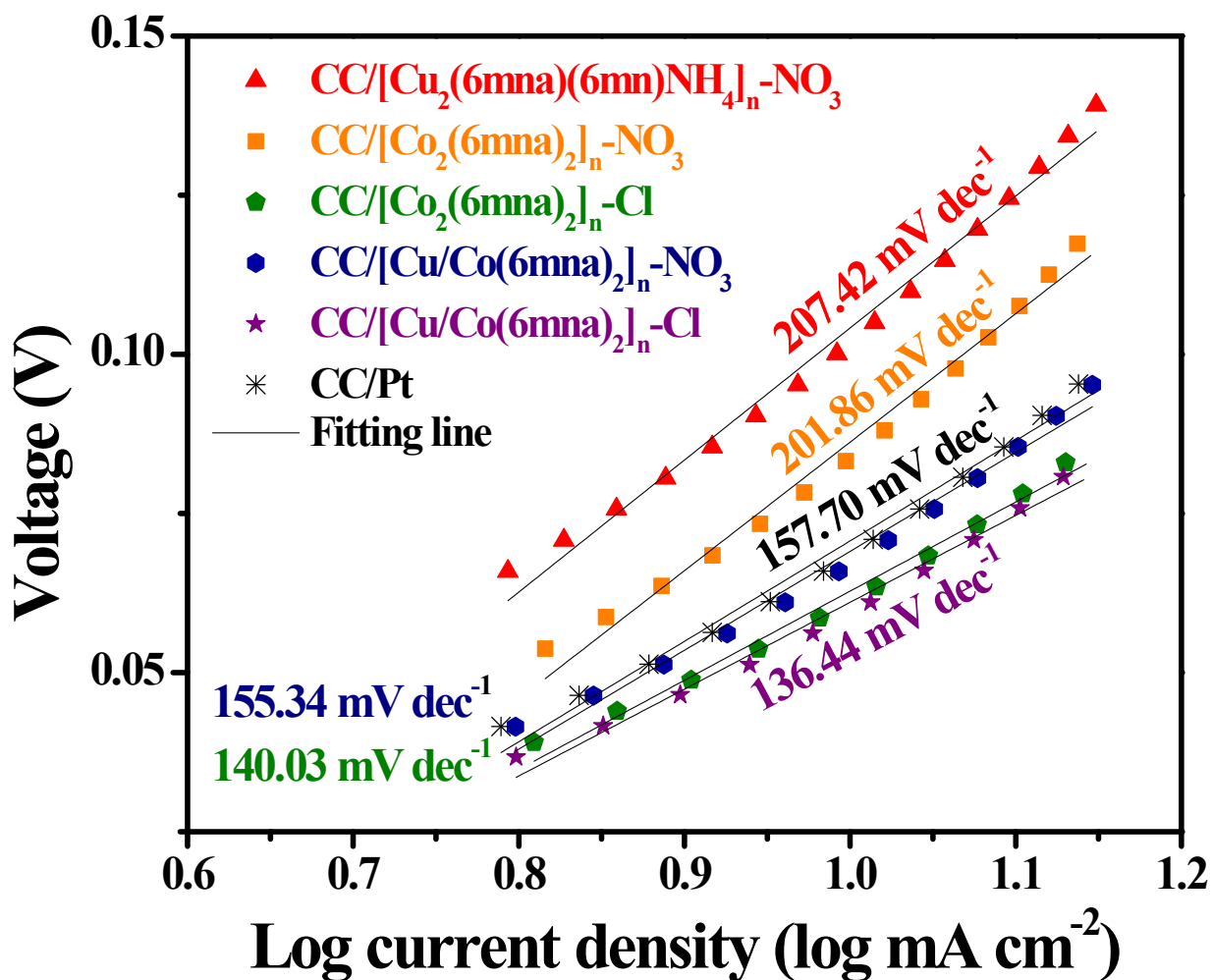


Fig. S17
electrolyte.

Tafel polarization V - $\log J$ plots for various electrodes, measured in an iodide-based

References:

1. C.-T. Li, F.-L. Wu, C.-J. Liang, K.-C. Ho, J. T. Lin, *J. Mater. Chem. A*, **2017**, *5*, 7586-7594.
2. Y. Saygili, M. Soderberg, N. Pellet, F. Giordano, Y. Cao, A. B. Munoz-Garcia, S. M. Zakeeruddin, N. Vlachopoulos, M. Pavone, G. Boschloo, L. Kavan, J. E. Moser, M. Gratzel, A. Hagfeldt, M. Freitag, *J. Am. Chem. Soc.*, **2016**, *138*, 15087-15096.
3. X. Cui, Z. Xie, Y. Wang, *Nanoscale*, **2016**, *8*, 11984-11992.
4. S. Huang, S. Li, Q. He, H. An, L. Xiao, L. Hou, *Appl. Surf. Sci.*, **2019**, *476*, 769-777.
5. C. Xu, J. Zhang, X. Qian, W. Wu, J. Yang, L. Hou, *Electrochim. Acta*, **2018**, *289*, 448-458.
6. W. Wang, Q. Cui, D. Sun, Q. Yang, J. Xu, W. Liao, X. Zuo, H. Tang, G. Li, S. Jin, *J. Mater. Chem. C*, **2021**, *9*, 7046-7056.
7. M. Sun, S. Yun, J. Dang, Y. Zhang, Z. Liu, D. Qiao, *Chem. Eng. J.*, **2023**, *458*, 141301.
8. A. S. A. Ahmed, W. Xiang, I. Saana Amiin, X. Zhao, *New J. Chem.*, **2018**, *42*, 17303-17310.
9. A. S. A. Ahmed, W. Xiang, Z. Li, I. S. Amiin, X. Zhao, *Electrochim. Acta*, **2018**, *292*, 276-284.
10. J. S. Kang, J. Kang, D. Y. Chung, Y. J. Son, S. Kim, S. Kim, J. Kim, J. Jeong, M. J. Lee, H. Shin, S. Park, S. J. Yoo, M. J. Ko, J. Yoon, Y.-E. Sung, *J. Mater. Chem. A*, **2018**, *6*, 20170-20183.
11. S.-L. Jian, Y.-J. Huang, M.-H. Yeh, K.-C. Ho, *J. Mater. Chem. A*, **2018**, *6*, 5107-5118.
12. J. Wu, W. Pan, Y. Lin, J. Zhu, Q.-S. Jiang, Y. Zhao, R. Ji, Y. Zhang, *J. Mater. Sci. Mater. Electron.*, **2020**, *31*, 12309-12316.
13. M.-S. Wu, J.-C. Lin, *Appl. Surf. Sci.*, **2019**, *471*, 455-461.
14. X. Jiang, H. Li, S. Li, S. Huang, C. Zhu, L. Hou, *Chem. Eng. J.*, **2018**, *334*, 419-431.
15. J. Ou, J. Xiang, J. Liu, L. Sun, *ACS Appl. Mater. Interfaces*, **2019**, *11*, 14862-14870.
16. T. Y. Chen, Y. J. Huang, C. T. Li, C. W. Kung, R. Vittal, K. C. Ho, *Nano Energy*, **2017**, *32*, 19-27.
17. Y.-Y. Wang, S.-M. Chen, R. Haldar, C. Wöll, Z.-G. Gu, J. Zhang, *Adv. Mater. Interfaces*, **2018**, *5*, 1800985.
18. A. N. Yang, J. T. Lin, C. T. Li, *ACS Appl. Mater. Interfaces*, **2021**, *13*, 8435-8444.